

# RSC Advances



This is an *Accepted Manuscript*, which has been through the Royal Society of Chemistry peer review process and has been accepted for publication.

*Accepted Manuscripts* are published online shortly after acceptance, before technical editing, formatting and proof reading. Using this free service, authors can make their results available to the community, in citable form, before we publish the edited article. This *Accepted Manuscript* will be replaced by the edited, formatted and paginated article as soon as this is available.

You can find more information about *Accepted Manuscripts* in the [Information for Authors](#).

Please note that technical editing may introduce minor changes to the text and/or graphics, which may alter content. The journal's standard [Terms & Conditions](#) and the [Ethical guidelines](#) still apply. In no event shall the Royal Society of Chemistry be held responsible for any errors or omissions in this *Accepted Manuscript* or any consequences arising from the use of any information it contains.

## Electrochemical synthesis of p-CuO thin films and development of a p-CuO/n-ZnO heterojunction and its application as selective gas sensor

Amrita Ghosh<sup>a</sup>, Bibhuti Bhushan Show<sup>b</sup>, Sugato Ghosh<sup>c</sup>, Nillohit Mukherjee<sup>c</sup>, Gautam Bhattacharya<sup>d</sup>, Swapan K. Datta<sup>c</sup> and Anup Mondal<sup>a\*</sup>

<sup>a</sup> Department of Chemistry, Indian Institute of Engineering Science & Technology (formerly Bengal Engineering and Science University), Shibpur, Howrah-711103, India

<sup>b</sup> Department of Chemistry, Jadavpur University, Kolkata-700032, India

<sup>c</sup> Centre of Excellence for Green Energy and Sensor Systems, Indian Institute of Engineering Science & Technology (formerly Bengal Engineering and Science University), Shibpur, Howrah-711103, India

<sup>d</sup> Department of Physics, RKM Vidyamandira, Belur, Howrah-711 202, India

**ABSTRACT:** p-CuO thin films have been synthesized on Indium Tin Oxide (ITO) coated glass substrates and on ZnO/ITO coated glass substrates using a new, simple, cost-effective electrochemical technique (Galvanic deposition) at room-temperature. X-ray Diffraction Technique (XRD) of the films show monoclinic phase of CuO and UV-vis spectroscopy of the CuO/ITO film shows indirect band-gap energy of about 1.85 eV. The surface morphology of CuO thin film consists of a c-axis grown regular macro porous network structure with deep cavities surrounded by thin solid walls, suitable for gas trapping and sensing. Current-Voltage characteristics of the formed p-CuO / n-ZnO film show good rectifying behavior. At 1 V reverse bias the leakage current density was as low as  $2 \times 10^{-9}$  A compared to the current  $1.2 \times 10^{-7}$  A at the same forward bias resulting in a forward-to reverse current ratio of about 60. The ideality factor of the diode was obtained to be quite as high of about 9.5. The frequency dependence of the small signal AC response in the both  $R_p - C_p$  and  $R_s - C_s$  mode of the fabricated heterojunction were measured at a reverse bias of 1.5 V. In the presence of 10000 ppm gas exposure for gases like CH<sub>4</sub>, H<sub>2</sub>S and CO, frequency dependent changes in AC responses are different for different gases. The

variation of the reactance of the fabricated device show different behaviour with exposure to different types of gases. The minimum in reactance occurs at different frequencies for different gases indicates the selectivity of the device for gas sensing.

**KEYWORDS:** Semiconductor, galvanic deposition, heterojunction, capacitive gas-sensing

## 1. INTRODUCTION

CuO is a narrow indirect band gap (1.2 eV) p-type semiconducting material. Recently, CuO nano materials have been recognized as an important material for versatile range of applications, such as optoelectronics,<sup>1</sup> catalysis,<sup>2</sup> gas sensing,<sup>3</sup> field emission,<sup>4</sup> reflectance measurements in the NIR region,<sup>5</sup> batteries<sup>6</sup> and photoelectrochemical cell.<sup>7</sup> Several reports are there on the fabrication of various CuO nano materials with various morphologies like nanorods,<sup>8</sup> nanoribbons,<sup>9</sup> nanoflowers,<sup>10</sup> nanosheets,<sup>11</sup> nanorings,<sup>12</sup> nanowires,<sup>13</sup> all having different optical, electrical and structural properties. Nanostructured metal oxide based thin films are receiving a growing attention for its utilization as gas sensor with enhanced accessible surface area. Among the variety of metal oxides, ZnO, CuO thin films based sensors have realized interest for its stability and cost-effectivity. An important area of recent research is the development of heterojunction based sensor for high selectivity and sensitivity. Few works have been done on the fabrication of both resistive type and capacitive type p-CuO/n-ZnO heterojunctions based gas-sensor which are sensitive to their environment, including

reducing gases and humidity.<sup>14,15</sup> However, no p-CuO/n-ZnO heterojunction based methane gas-sensor is reported so far to the best of our knowledge. Though, there are few reports on other semiconducting materials based heterojunction as non-capacitive type methane gas-sensors.<sup>16,17</sup> Thin film semiconducting materials generally have been made by sputtering,<sup>18</sup> spray pyrolysis,<sup>19</sup> electrochemical<sup>20</sup> and chemical bath deposition<sup>21</sup> methods.

Here, we report a new, simple and inexpensive electrochemical technique, called the galvanic technique to deposit thin films of CuO, firstly on ITO coated glass and then over ZnO thin films,<sup>22</sup> deposited on ITO coated glass. The utility of this process lies in its simplicity and overall ease of operation. Galvanostat /potentiostat as the external energy source is not required, as the overall cell potential acts as the driving force for the reaction. Here, room temperature (25°C) is the operating temperature. The process for thin-film deposition involves low setup cost and minimum energy consumption. This technique has been successfully used previously to deposit various other thin-film semiconductors<sup>22-24</sup> in our laboratory. Current-voltage measurements were carried out to study the rectifying behavior of the formed p-CuO / n-ZnO heterojunction and A.C. measurements were carried out to study the suitability of p-CuO / n-ZnO heterojunction for room temperature selective gas sensing using capacitive-mode.

## 2. EXPERIMENTAL DETAILS

### 2.1 Chemicals:

Cu(NO<sub>3</sub>)<sub>2</sub>·3H<sub>2</sub>O and L(+)-Tartaric acid GR were purchased from MERCK, ZnSO<sub>4</sub>·7H<sub>2</sub>O from BDH and 30% W/V H<sub>2</sub>O<sub>2</sub> from Fisher Scientific. All the chemicals were used without further purification. Millipore water was used in all experiments.

## 2.2 Preparation of CuO thin film:

### A. Preparation of solution:

To an aqueous 0.01 (M)  $\text{Cu}(\text{NO}_3)_2 \cdot 3\text{H}_2\text{O}$  solution, 2.5 ml of 0.01 (M) of GR L (+)-Tartaric acid solution was added as a complexing agent. The solution was stirred for about 5 mins. The resulting solution was made around 99 ml with DI water and finally 1 ml of 30% W/V  $\text{H}_2\text{O}_2$  were added as an oxidizing agent. The pH of the working solution was in the range 5-6. This was found to be optimum for producing good CuO films.

### B. Cell set up:

At first, ITO coated glass substrates were cleaned with detergent and then dipped into chromic acid solution for about 10 minutes and washed thoroughly with water. A Zn rod (99.9% purity) and a cleaned ITO coated glass substrate were dipped into the working solution and short-circuited externally through a Cu wire. Here, Zn rod (easily oxidisable) acts as a self-decaying anode and the ITO coated glass substrate as cathode. The working solution was stirred continuously using a magnetic stirrer. The same set up was used to develop CuO thin film on ZnO coated ITO substrates. Thin films of ZnO were deposited from a zinc sulfate bath on ITO surface following the previously reported work of our laboratory.<sup>22</sup>

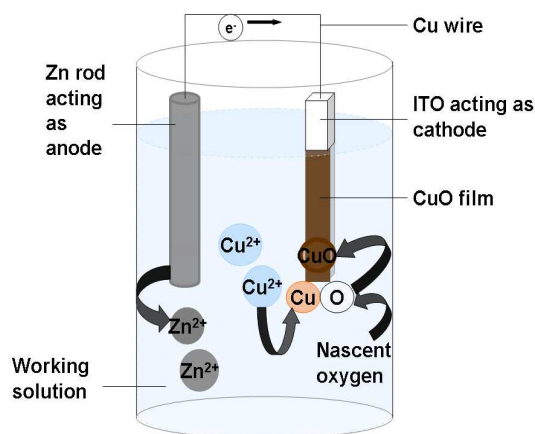


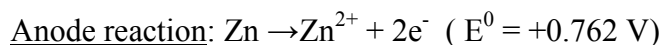
**Fig. 1** Schematic representation of the 'Galvanic Deposition' set up.

### 2.3 Characterization:

The deposited films were characterized by their optical, structural, morphological and electrical properties. Thicknesses of the films were determined gravimetrically using a digital balance (Mettler). The UV-vis spectra of the thin films were taken by a 'JASCO V-530' UV-vis spectrophotometer. X-ray diffraction patterns were recorded by an X-ray diffractometer (Seifert P3000, Cu K $\alpha$  radiation  $\lambda = 1.54 \text{ \AA}$ ). The morphology of the thin films was studied using a field-emission scanning electron microscope (FESEM) (JEOL JSM-6700F). Electrical characterizations were carried out using DC I-V and AC measurements. Since, ITO (indium doped tin oxide) coated glass substrates on which depositions were carried out is a highly conducting material, it was used as the bottom contact for electrical measurements of the films. Top contacts were taken from the CuO layer for both p-CuO thin films on ITO and p-CuO/n-ZnO heterojunction on ITO. Ag-Pd is used as the top metal contact keeping the area of contacts ( $\sim 0.20 \text{ sq.cm}$ ) and thicknesses of both ZnO and CuO ( $0.30 \mu\text{m}$  for each layer) constant for all DC and AC measurements. The DC voltage was applied along the thickness of the films using a KITHLEY 4200 instrument. AC measurements were carried out using an AGILENT 4284A precision LCR meter.

## 3. RESULTS AND DISCUSSION

### 3.1 Deposition chemistry of CuO film:



Cathode reaction:  $\text{Cu}^{2+} + 2\text{e}^{-} \rightarrow \text{Cu}$  ( $E^0 = -0.337 \text{ V}$ )

$E^0$  represents oxidation potential.

Zn being easily oxidisable acts as anode. It is clear that  $\text{Zn} + \text{Cu}^{2+} \rightarrow \text{Cu} + \text{Zn}^{2+}$  is a spontaneous reaction. To avoid deposition of metallic Cu at cathode,  $\text{H}_2\text{O}_2$  was added in solution. In presence of light,  $\text{H}_2\text{O}_2$  decomposes as  $2\text{H}_2\text{O}_2 = 2\text{H}_2\text{O} + \text{O}_2$ . Nascent oxygen produced in situ oxidizes Cu and gets deposited as CuO, instead of metallic Cu, on ITO. Also, the pH of the solution is important to avoid deposition of free Cu. A deposition rate of  $\sim 3.34 \text{ \AA}$  per second was achieved with a total thickness of around  $5000 \text{ \AA}$  within 25 minutes of deposition. Thicker deposition can be achieved with longer deposition time.

### 3.2 Structural characterization:

#### **XRD analysis:**

X-ray diffraction measurements of the films were carried out to ascertain the formation of CuO and to determine the phase. XRD pattern of an as-deposited CuO thin film on ITO coated glass by the galvanic technique has been presented in Figure 2a. Diffraction from CuO thin film matches with the results of the JCPDS card no. 89-2531, showing a monoclinic phase for CuO, with diffraction from (002), (111), ( $\bar{1}$ 13) planes. Figure 2b shows the XRD patterns for as-deposited CuO on galvanically deposited ZnO films coated over ITO glass.

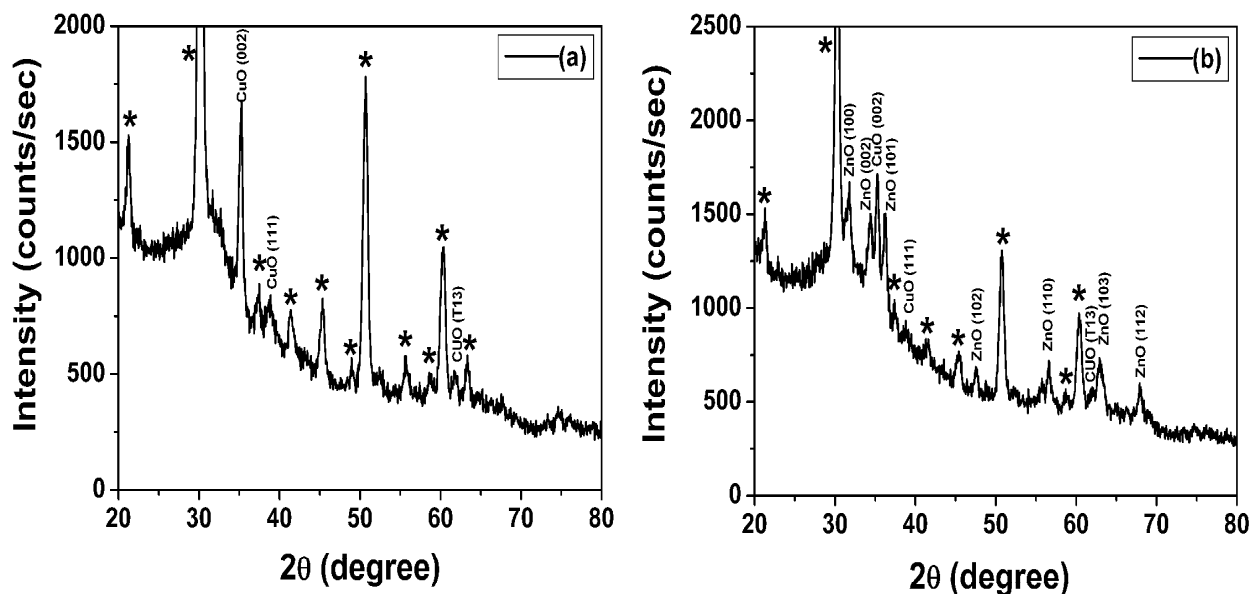


**Fig. 2** X-ray diffraction patterns of (a) as-deposited CuO film on ITO (b) as-deposited CuO film on ZnO coated ITO. \* represents peaks due to ITO.

### 3.3 Optical characterization:

The UV-vis spectra of the CuO thin films were taken by a 'JASCO V-530' UV-vis spectrophotometer. As-deposited CuO thin films show a sharp change in the absorption, giving rise to a band-edge around 560 nm. However, on annealing in air at around 300°C, a shift in the absorption edge towards longer wavelength occurs. CuO is known to be an indirect band gap semiconductor. Hence, optical

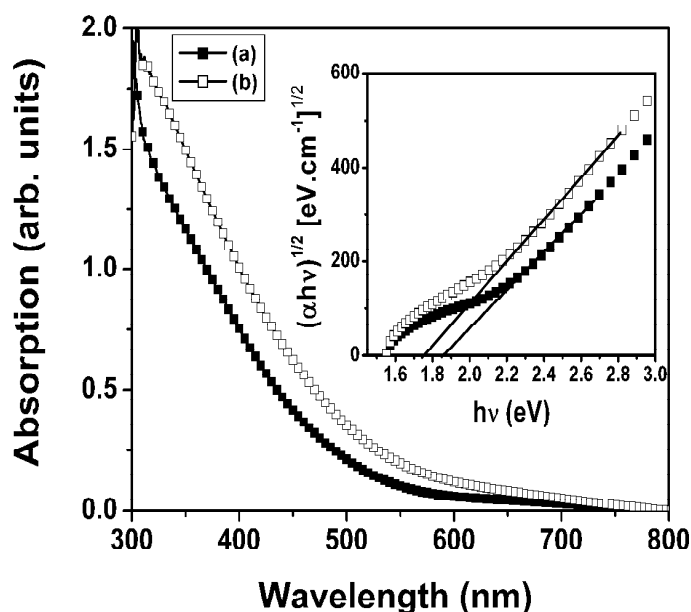


**Fig. 3** UV-vis spectra of (a) as-deposited CuO film, deposited from aqueous  $\text{Cu}(\text{NO}_3)_2$  bath at  $25^\circ\text{C}$  (corresponding Tauc plot in inset showing band gap of 1.85 eV) and (b) same film annealed in air at  $300^\circ\text{C}$  (band gap 1.75 eV).

band gaps were calculated by plotting  $(\alpha h\nu)^{1/2}$  versus  $h\nu$  and extrapolating the linear portion of the curves to  $(\alpha h\nu)^{1/2} = 0$ , where  $h\nu$  is the energy of photon and  $\alpha$  is the absorption coefficient.

CuO is a p-type semiconducting material with room temperature indirect band gap energy of about 1.2 eV for the bulk systems. The UV-vis spectrum of the material shows significant amount of blue-shift in the band gap energy, most likely due to quantum confinement effect shown by the as-deposited CuO nano-crystals. As a result, energy gap between the conduction band and valence band increases, resulting in a blue shift in the band gap value for the as-deposited nano-crystals. However, on annealing, the band gap

energy value decreases from **1.85 eV** to **1.75 eV**. The small crystallites of CuO fuse to form larger grains on annealing. This results in a red shift in the absorption band edge, and consequently, to a decrease in the energy band gap value.

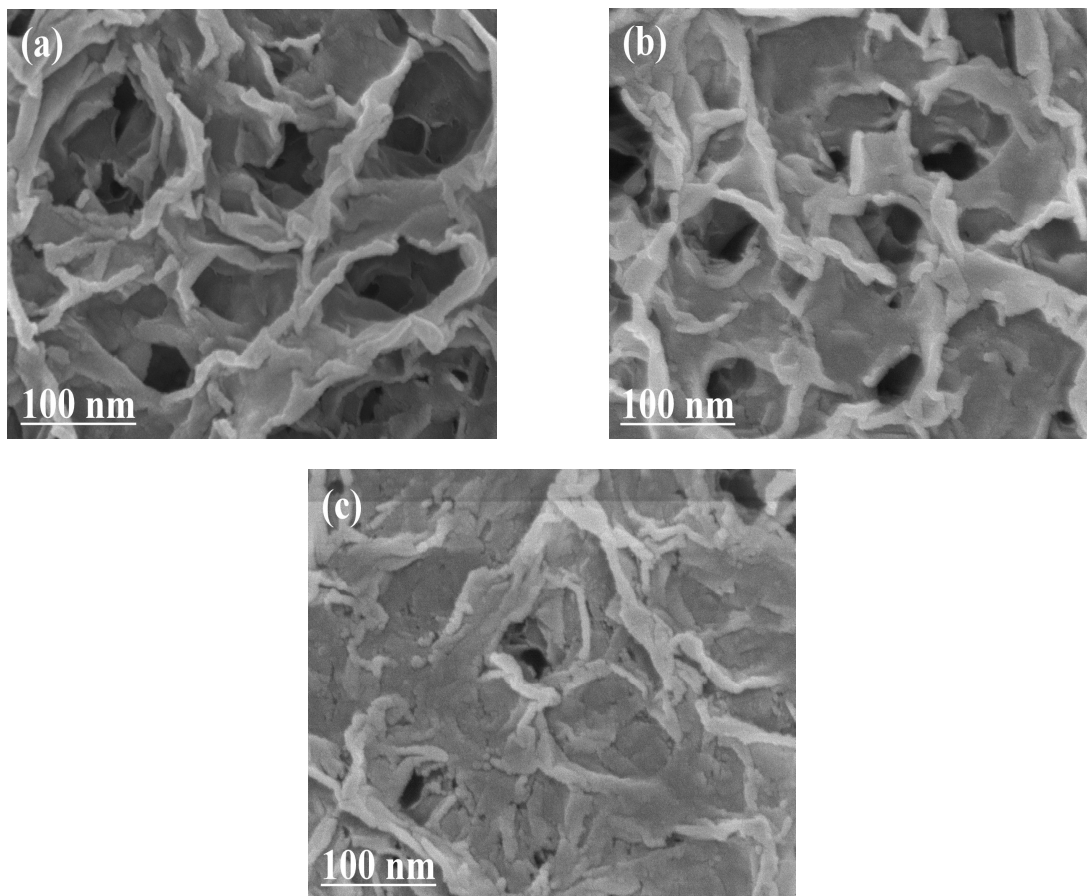
### 3.4 FESEM images:

Figure 4a represents the FESEM image of an as-deposited CuO thin film on ITO coated glass. From the figure it can be observed that the surface morphology of CuO thin film consists of a c-axis grown regular macroporous network structure with deep cavities surrounded by thin solid walls. The pore diameters are around 150 – 350 nm.

Figure 4b represents the surface morphology of CuO thin film deposited on ZnO thin film. The same feature is repeated, however, in this case, the macroporous structure seems to be more densely packed and the average pore diameter decreases to 150 – 250 nm.

ITO has a higher conductivity in comparison to ITO-ZnO structure and the surface is much smoother for ITO than ZnO, therefore deposition of CuO over ITO is much faster than deposition of CuO over ZnO. Fast deposition leads to relatively less compact CuO film while a slow and steady deposition of CuO over a rough and much resistive ZnO layer leads to a much more compact CuO film. This is reflected in figures 4a and 4b where the density of the deposited CuO is less (arising from larger pore diameter) over ITO, compared to more densely deposited CuO over ZnO film (pore diameter being less). Figures 4c represents the surface morphology of air annealed CuO film deposited over ZnO film. It can be clearly observed that on annealing, a distinct change takes place for

the CuO film. The thin vertical walls which formed the pores start breaking down, giving rise to much shallow pores and also to a loss in the number of pores per unit area, resulting in a flatter appearance of the surface morphology of CuO film, with pore diameters decreasing to 75 -150 nm.



**Fig. 4** FESEM images of (a) as-deposited CuO film on ITO ( b) as-deposited CuO film on ZnO coated ITO ( c) annealed (300°C for 15 minutes) CuO film on ZnO coated ITO.

### 3.5 Electrical characterization:

#### 3.5.1 Electrical characterization of CuO thin films on ITO:

DC I-V characteristics were measured for p-CuO thin films of thickness 0.2 $\mu$ m coated on ITO and the curves for both as grown and heat treated showed almost linear

characteristics, indicating near ohmic behavior. The film resistivity was calculated to be of the order of  $2 \times 10^6 \Omega\text{-m}$ . The high resistivity appears to be due to the porous structure as can be seen from Figure 4.

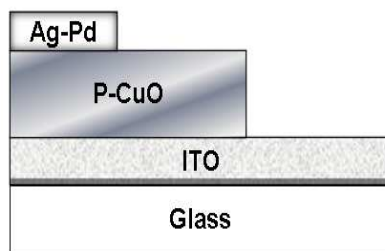


Fig. 5 Schematic of p-CuO on ITO for obtaining I-V characteristics.

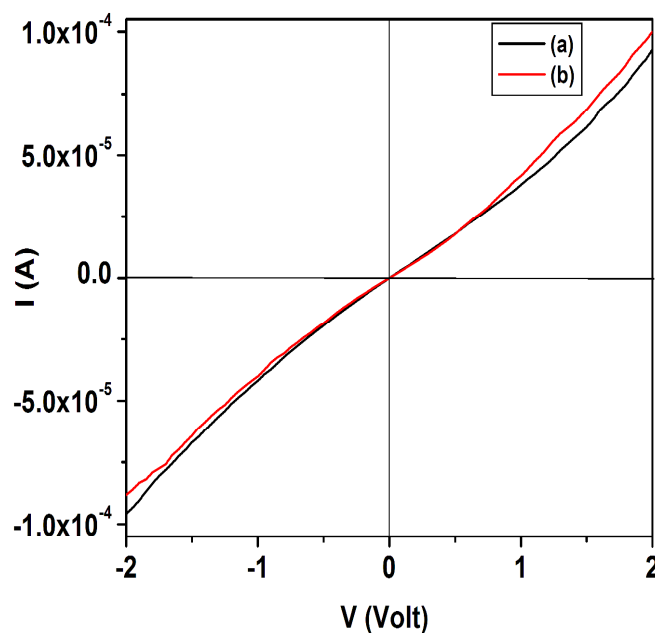
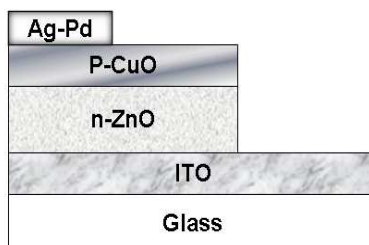


Fig. 6 Forward and reverse bias I-V graphs of CuO thin films on ITO (a) as-deposited (b) heat treated (at  $300^\circ\text{C}$ ) samples.

### 3.5.2 Electrical Characterization of p-CuO/n-ZnO heterojunction:

#### 3.5.2.1 DC I-V Characteristics:

I-V measurements were carried out at room temperature [Figure 7]. The samples were kept in the dark during measurements.



**Fig. 7** Schematic of the p-CuO/n-ZnO structure for obtaining I-V characteristics.

The measured I-V characteristics of the p-CuO / n-ZnO heterojunction, before and after annealing in air at 300 °C for 15 minutes have been presented in Figures 8 (a) and 8 (b). As can be seen from the figures, the rectifying behavior of the I-V of the heterojunction diode is evident. At 1 V reverse bias the leakage current density was as low as  $2 \times 10^{-9}$  A compared to the current  $1.2 \times 10^{-7}$  A at the same forward bias resulting in a forward-to-reverse current ratio of about 60.

Moreover, at high forward bias, the current varies slowly than that predicted from the exponential behaviour and I-V curves become almost linear. This suggests that the heterojunction diode behavior is controlled by the bulk resistances of the materials of CuO and ZnO,<sup>25</sup> in addition to the junction properties. It is also found that the current through the heterojunction increases on heat treatment implying a reduction in the bulk resistance of the sample.

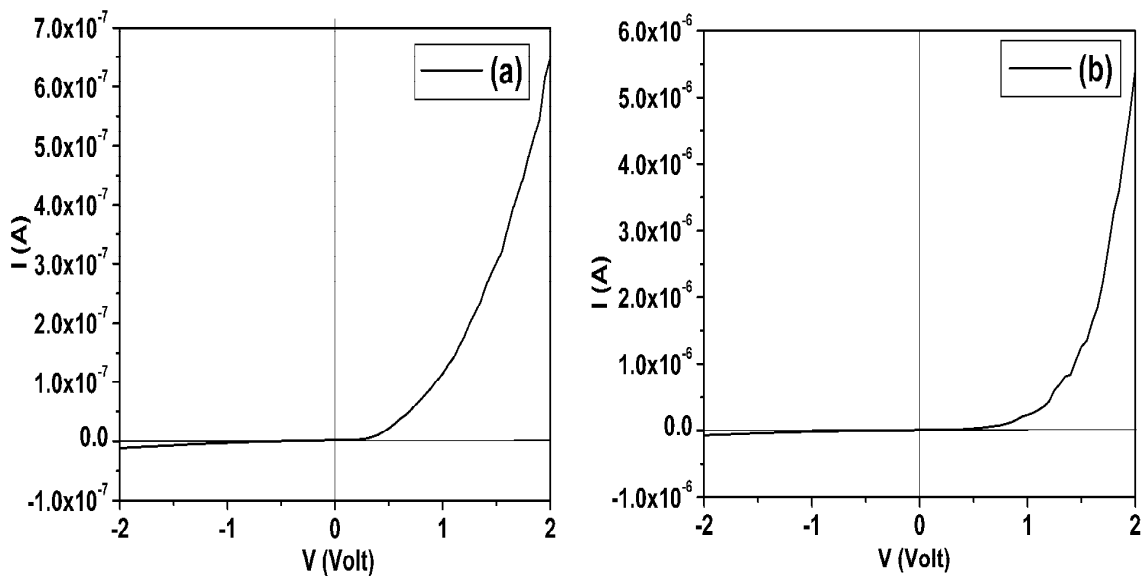


**Fig. 8** Forward and reverse bias I-V characteristics of CuO/ZnO heterojunction, (a) as-deposited and (b) heat treated (at 300°C for 15 minutes) samples.

The relationship between the current and the applied voltage across the heterojunction can be expressed as

$$I = I_0 \left( e^{\frac{q(V-IR_b)}{\eta kT}} - 1 \right) \text{ ----- (1)}$$

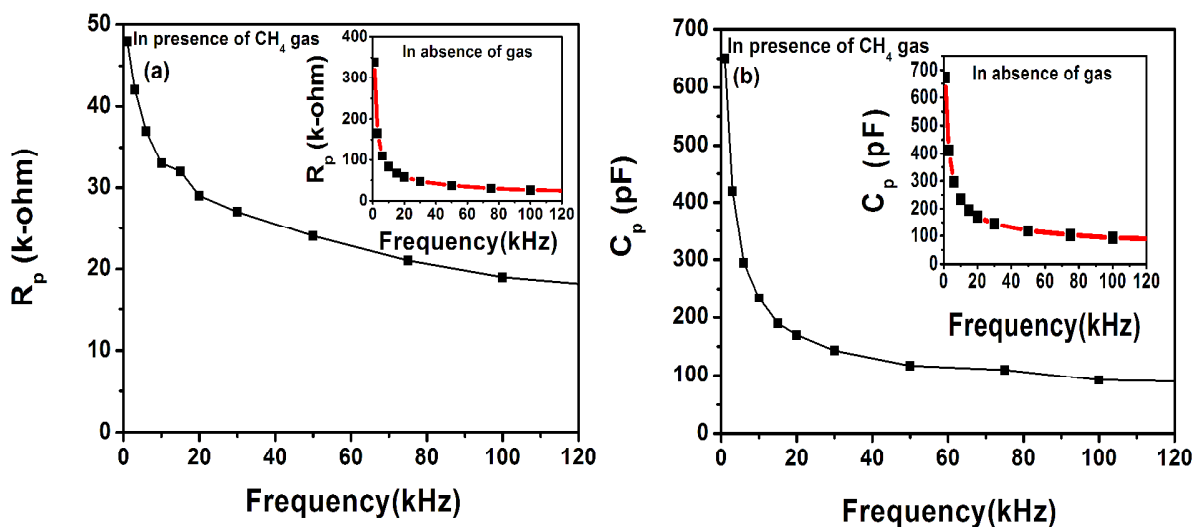
where, the pre-exponential factor  $I_0$  is the reverse saturation current,  $\eta$ , is the diode quality factor,  $V$  is the applied voltage across the sample and  $R_b$  is the series resistance included to account for the bulk resistance of the sample. An analysis of the linear I-V data in the high forward bias region (1.5 V – 2.0 V) shows a series resistance of about 1.2- 1.4 M $\Omega$  for the as-deposited samples which decreases by an order of magnitude on heat treatment. From the curve fitting of the I-V data, the built in potential of the heterojunction of the annealed sample was found to be about 1.5 V compared to 1.1 V for as deposited samples which is fairly close to the value of 1.54 V reported by others.<sup>25-26</sup>

The ideality factor was obtained to be quite as high of about 9.5 for both as-deposited and

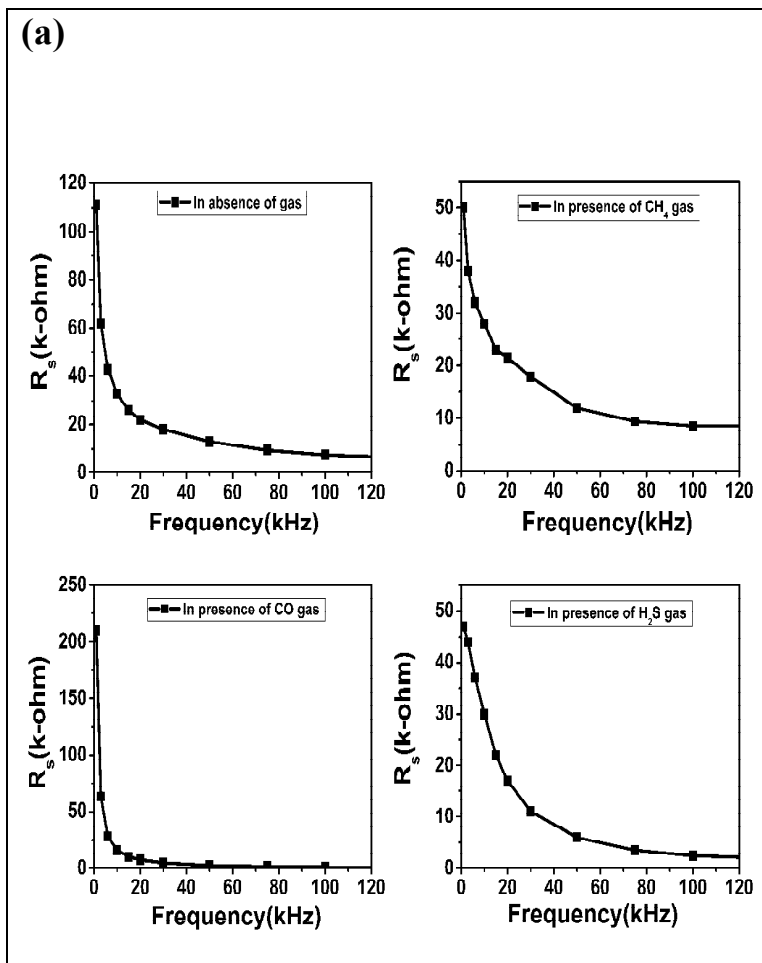
annealed samples. High ideality factor of about 7 was also observed by others for CuO-ZnO heterojunctions.<sup>26</sup> One plausible reason for such high value of the ideality factor is that the current transport mechanism is dominated by both interface traps and space charge at the heterojunction.

### 3.5.2.2 Frequency dependence of reactance of the heterojunction:

The frequency dependence of the small signal AC response in the both  $R_p - C_p$  (resistance and capacitance in parallel) for samples in absence of gas and in presence of  $\text{CH}_4$  gas and  $R_s - C_s$  (resistance and capacitance in series) mode of the fabricated heterojunction (as-deposited p-CuO /n-ZnO) for sample in absence of gas, and in presence of  $\text{CH}_4$ , CO and  $\text{H}_2\text{S}$  gases are shown respectively in figures 9(a)-9(b) and 10(a)-10(b) at a reverse bias of 1.5 V.



**Fig. 9** The frequency dependence of the small signal AC response in the (a) $R_p$  -(b)  $C_p$  mode of the fabricated as-deposited p-CuO / n-ZnO heterojunction both in absence(inset) and presence of gas.



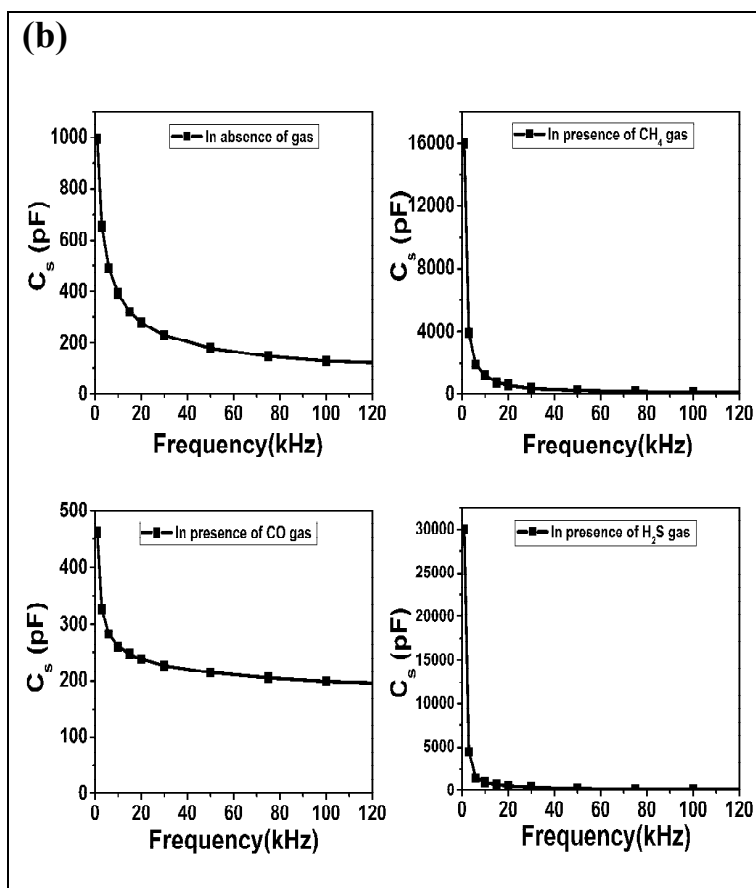


**Fig. 10** The frequency dependence of the small signal AC response in the (a) $R_s$  -(b)  $C_s$  of the fabricated as-deposited p-CuO / n-ZnO heterojunction both in absence and presence of different gases.

It is found from these figures that  $R_p$  and  $C_p$  as well as  $R_s$  and  $C_s$  monotonically decrease with increase in frequency and tend to become constant at high frequencies. These results can be qualitatively interpreted in terms of an equivalent circuit<sup>27</sup> where the sample can be modeled as a diode heterojunction having composed of a parallel combination of the high resistance  $R_j$  at reverse bias, depletion capacitance,  $C_D$ , and a combination of series connected capacitance and resistance elements,  $C_t$  and  $R_t$  due to the interface states.

It appears that at higher frequencies, the interface states cannot follow the AC signal<sup>28</sup> and consequently cannot contribute much to the capacitance. It indicates that the interface states are responsible for the observed frequency variation in  $C_p$ .

A plot of the reactance ( $X_s = -1/\omega C_s$ ) of the device with frequency is shown in Figure 11. The reactance of the samples without gas exposure increases monotonically with increase in frequency and becomes almost constant at higher frequencies [Fig. 11(a)].

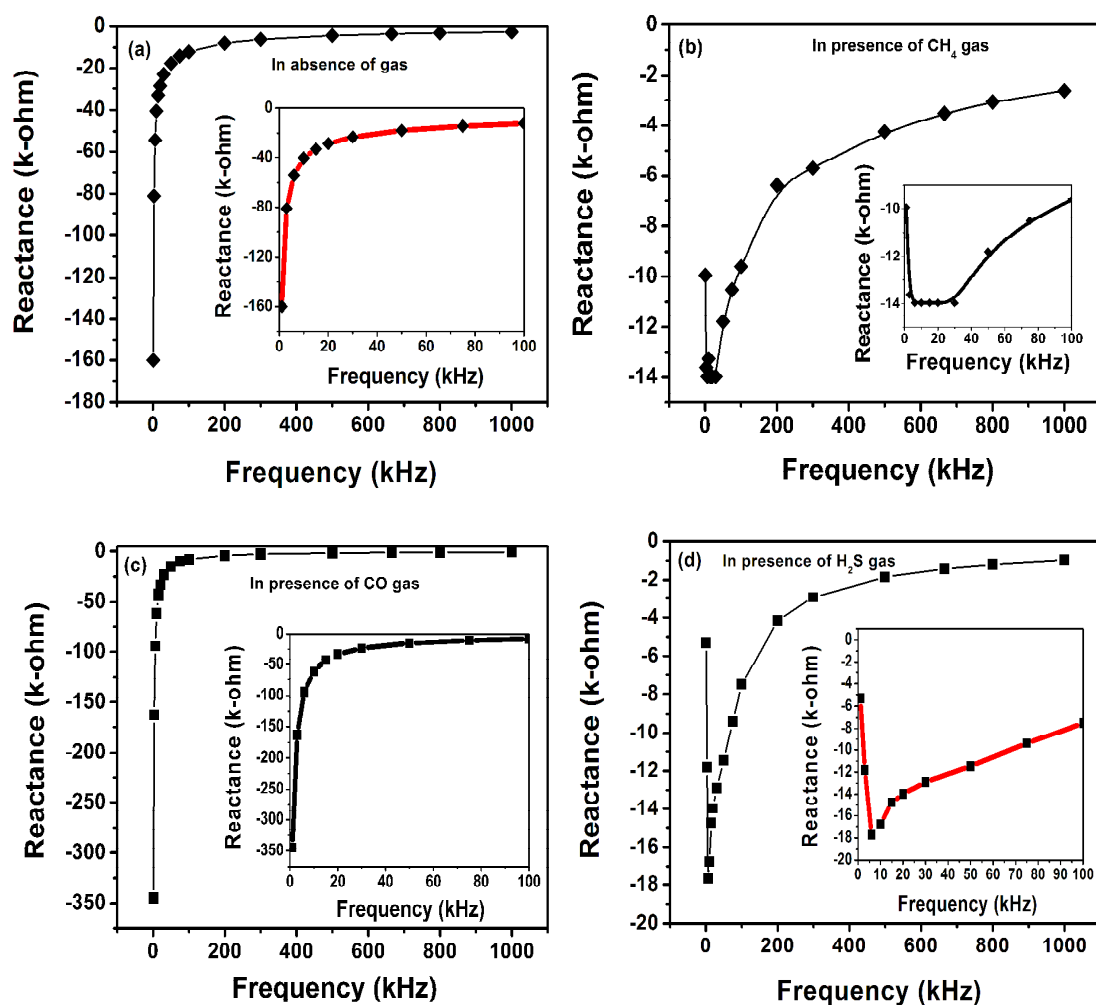


**Fig. 11** Frequency dependence of reactance of the heterojunction in (a) absence of gas (b) presence of CH<sub>4</sub> gas (c) CO gas (d) H<sub>2</sub>S gas (inset carries images with significant zone).

However, the reactance behaviour of the samples are different for exposure to different gases. While the reactance of the samples increases on exposure to CO, the reactance of the samples decreases on exposure to other gases (CH<sub>4</sub> and H<sub>2</sub>S).

In the presence of 10000 ppm methane gas exposure, R<sub>p</sub> decreases significantly at low frequencies, while almost no change is observed at higher frequencies (300 kHz – 1 MHz). On the other hand, C<sub>p</sub> changes very little on gas exposure. Plots of reactance (calculated from R<sub>p</sub> and C<sub>p</sub>) of the device with frequency are shown in **Fig. S1.** and **Fig. S2.** Reactance value matches exactly with that calculated from C<sub>s</sub> (shown in **Fig. 11 (a) & (b)**).

In terms of R<sub>p</sub> and C<sub>p</sub>, the values of R<sub>s</sub> and C<sub>s</sub> are given by

$$R_s = \frac{R_p}{1 + \omega^2 R_p^2 C_p^2} \quad \text{and} \quad C_s = C_p \left(1 + \frac{1}{\omega^2 R_p^2 C_p^2}\right) \quad (2)$$

Small decrease of R<sub>s</sub> is observed, while C<sub>s</sub> increases significantly at lower frequencies on gas exposure. These changes can be explained on the basis of equation (2) and measured R<sub>p</sub>, by assuming a large increase of R<sub>p</sub> on gas exposure.<sup>29</sup>

The frequency dependence of reactance of the heterojunction on gas exposure to H<sub>2</sub>S and methane [Figure 11 (b), (d)] shows a minimum instead of monotonic increase, though no such minimum is observed for CO exposure. The minimum is extremely sharp for H<sub>2</sub>S occurring at around 6 kHz, while for CH<sub>4</sub>, the minimum is almost a broadband in the range of 6 - 30 kHz. This indicates the proof-of-concept for the suitability of the fabricated device for gas sensing.

In analogy with the definition of sensitivity of conductivity mode gas sensing devices, we can define the sensitivity of capacitive mode gas sensing at each frequency as the fractional change in reactance on gas exposure with respect the reactance without gas

exposure. Sensitivity as a function of frequency is shown in Fig. 12 for different frequencies for different types of gas exposure.

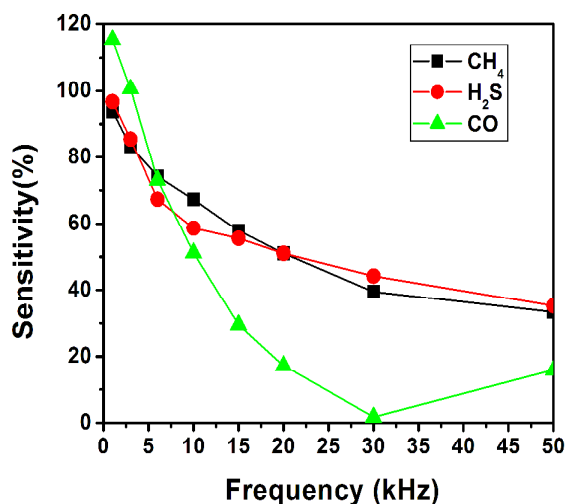


**Fig. 12** Frequency dependence of sensitivity of the heterojunction in presence of CH<sub>4</sub>, CO, H<sub>2</sub>S gas.

The density of interface states is dependent on the processing parameters of the heterojunction<sup>30</sup> and the frequency tunable sensing property of the minimum reactance together with the sensitivity at this frequency may be utilized for selective gas detection by CuO – ZnO gas sensors.

The detailed device characterization in respect to sensitivity for different ppm levels of gas exposure, selectivity, the transient response to different gases are in progress.

#### 4. CONCLUSION

p-CuO thin films have been successfully synthesized both on conducting and semi-conducting substrates using a new, cost-effective galvanic technique. The morphology we have obtained by this process is a c-axis grown regular macro porous network structure with deep cavities surrounded by thin solid walls, very suitable for gas-trapping and

sensing. I-V characteristics of the p-CuO/n-ZnO heterojunction show good rectifying behaviour with high ideality factor. The formed p-CuO (as-deposited) / n-ZnO heterojunction have been found to behave differently in terms of reactance at different frequencies for exposure to gases like methane, H<sub>2</sub>S and CO. The fabricated heterojunction appears to be suitable frequency selective gas sensing device for different types of gases.

## REFERENCES

- 1 S. Manna, K. Das and S. K. De, *ACS Appl. Mater. Interfaces*, 2010, **2**, 1536.
- 2 S. Reddy, B. E. Kumara Swamy and H. Jayadevappa, *Electrochimica Acta*, 2012, **61**, 78.
- 3 M. Yang, J. He, X. Hu, C. Yan and Z. Cheng, *Environ. Sci. Technol.*, 2011, **45**, 6088.
- 4 Y. W. Zhu, T. Yu, F. C. Cheong, X. J. Xu, C. T. Lim, V. B. C. Tan, J. T. L. Thong and C. H. Sow, *Nanotechnology*, 2005, **16**, 88.
- 5 K. M. Shrestha, C. M. Sorensen and K. J. Klabunde, *J. Phys. Chem. C*, 2010, **114**, 14368.
- 6 S. Gao, S. Yang, J. Shu, S. Zhang, Z. Li and K. Jiang, *J. Phys. Chem. C*, 2008, **112**, 19324.
- 7 C. Y. Chiang, J. Epstein, A. Brown, J. N. Munday, J. N. Culver and S. Ehrman, *Nano Lett.*, 2012, **12**, 6005.
- 8 W. Wang, Z. Liu, Y. Liu, C. Xu, C. Zheng and G. Wang, *Appl. Phys. A*, 2003, **76**, 417.
- 9 B. Liu and H. C. Zeng, *J. Am. Chem. Soc.*, 2004, **126**, 8124.
- 10 M. Basu, A. K. Sinha, M. Pradhan, S. Sarkar, A. Pal and T. Pal, *Chem. Commun.*, 2010, **46**, 8785.
- 11 F. Zhang, A. Zhu, Y. Luo, Y. Tian, J. Yang and Y. Qin, *J. Phys. Chem. C*, 2010, **114**, 19214.
- 12 X. Wang, G. Xi, S. Xiong, Y. Liu, B. Xi, W. Yu and Y. Qian, *Cryst. Growth Des.*, 2007, **7**, 930.

- 13 J. Hu, D. Li, J. G. Lu and R. Wu, *J. Phys. Chem. C*, 2010, **114**, 17120.
- 14 L. Yang, C. Xie, G. Zhang, J. Zhao, X. Yu, D. Zeng and S. Zhang, *Sensors and Actuators B*, 2014, **195**, 500.
- 15 S. J. Jung and H. Yanagida, *Sensors and Actuators B*, 1996, **37**, 55.
- 16 P. Bhattacharyya, G. P. Mishra and S. K. Sarkar, *Microelectronics Reliability*, 2011, **51**, 2185.
- 17 B. Matveev, M. Aidaraliev, G. Gavrilov, N. Zotova, S. Karandashov, G. Sotnikova, N. Stus', G. Talalakin, N. Il'inskaya and S. Aleksandrov, *Sensors and Actuators B*, 1998, **51**, 233.
- 18 P. Samarasekara, M. A. K. Mallika Arachchi, A. S. Abeydeera, C. A. N. Fernando, A. S. Disanayake and R. M. G. Rajapakse, *Bull. Mater. Sci.*, 2005, **28**, 483.
- 19 J. Morales, L. Sa'nchez, F. Marti'n, J. R. Ramos-Barrado and M. Sa'nchez, *Thin Solid Films*, 2005, **474**, 133.
- 20 V. Dhanasekaran, T. Mahalingam, R. Chandramohan, J. K. Rhee and J. P. Chu, *Thin Solid Films*, 2012, **520**, 6608.
- 21 F. Bayansal, S. Kahraman, G. C. ankaya, H. A. C, etinkara, H. S. Guder and H. M. C, akmak, *Journal of Alloys and Compounds*, 2011, **509**, 2094.
- 22 N. Mukherjee, S. F. Ahmed, K. K. Chattopadhyay, A. Mondal, *Electrochimica Acta*, 2009, **54**, 4015.
- 23 U. Madhu, N. Mukherjee, N. R. Bandyopadhyay and A. Mondal, *Indian J. Pure Appl. Phys.*, 2007, **45**, 226.

- 24 N. Mukherjee, S. F. Ahmed, D. Mukherjee, K. K. Chattopadhyay and A. Mondal, *phys. stat. sol. (c)*, 2008, **5**, 3458.
- 25 F. Özyurtkus, T. Serin and N. Serin, *J OPTOELECTRON ADV M*, 2009, **11**, 1855.
- 26 A. Zainelabdin, S. Zaman, G. Amin, O. Nur and M. Willander, *Appl. Phys. A: Mater. Sci. Process.*, 2012, **108**, 921.
- 27 R. Romero, M. C. López, D. Leinen, F. Mart´ın and J. R. Ramos-Barrado, *Mater. Sci. Eng., B*, 2004, **110**, 87.
- 28 Z. Ahmad, M. H. Sayyad, K. S. Karimov, M. Saleem and M. Shah, *ACTA PHYS POL A*, 2010, **117**, 493.
- 29 S. Kwon, S. Aygun and D. P. Cann, *Sensor Lett.*, 2005, **3**, 258.
- 30 Y. Ushio, M. Miyayama and H. Yanagida, *Sensors and Actuators B*, 1994, **17**, 221.

## ACKNOWLEDGMENTS

This work was financially supported by DST, India (project no. ID/Sensor-New/05/2010-11). A.Ghosh is grateful to DST (India) for project fellowship. The authors also acknowledge All India Council for Technical Education and U.G.C.-S.A.P. (India) for providing instrumental facilities to the Department of Chemistry, IEST, Shibpur, India.

## Table of Contents entry

The fabricated p-CuO / n-ZnO heterojunction senses gases selectively at room temperature.

